RSC Advances

PAPER

View Article Online
View Journal | View Issue



Cite this: *RSC Adv.*, 2022, **12**, 8435

# Fluorescence detection of malachite green and cations ($Cr^{3+}$, $Fe^{3+}$ and $Cu^{2+}$) by a europium-based coordination polymer†

Ya-Jie Kong,[a] Guo-Zheng Hou,[a] Zhao-Ning Gong,[a] Feng-Tan Zhao[a] and Li-Juan Han *[ab]

Received 6th January 2022
Accepted 9th March 2022

DOI: 10.1039/d2ra00077f

rsc.li/rsc-advances

Due to remarkable fluorescence characteristics, lanthanide coordination polymers (CP) have been widely employed in fluorescence detection, but it is rarely reported that they act as multifunctional luminescent probes dedicated to detecting malachite green (MG) and various metal ions. A europium-based CP fluorescent probe, $Eu(PDCA)_2(H_2O)_6$ (PDCA = 2,6-pyridinedicarboxylic acid), has been synthesized and exhibited excellent recognition ability for malachite green and metal cations ($Cr^{3+}$, $Fe^{3+}$ and $Cu^{2+}$) among 11 metal cations, 13 anions and six other compounds. The recognition was achieved by fluorescence quenching when MG, $Cr^{3+}$, $Fe^{3+}$ and $Cu^{2+}$ were added to a suspension of $Eu(PDCA)_2(H_2O)_6$ respectively. $Eu(PDCA)_2(H_2O)_6$ is a multifunctional luminescent probe, and displayed high quenching efficiencies $K_{sv}$ ($2.10 \times 10^6$ $M^{-1}$ for MG; $1.46 \times 10^5$ $M^{-1}$ for $Cr^{3+}$; $7.26 \times 10^5$ $M^{-1}$ for $Fe^{3+}$; $3.64 \times 10^5$ $M^{-1}$ for $Cu^{2+}$), and low detection limits (MG: 0.039 μM; $Cr^{3+}$: 0.539 μM; $Fe^{3+}$: 0.490 μM; $Cu^{2+}$: 0.654 μM), presenting excellent selectivity and sensitivity, especially for MG. In addition, $Eu(PDCA)_2(H_2O)_6$ was also made into fluorescent test strips, which can rapidly and effectively examine trace amounts of MG, $Cr^{3+}$, $Fe^{3+}$ and $Cu^{2+}$ in aqueous solutions. This work provides a new perspective for detecting malachite green in fish ponds and heavy metal ions in waste water.



## 1. Introduction

Malachite green (MG) is a triphenylmethane compound, exists as green crystals and is easily soluble in water. It is an industrial dye and used for dyeing wool, paper and other materials. In the past, malachite green has been utilized as a fungicide in the aquaculture field to control parasites, fungi and bacterial infections in aquatic products.[1,2] However, later studies showed that malachite green and its metabolites have obvious residues and toxicity in aquatic animals, which can cause cancer, teratogenicity and mutation.[3,4] In the field of pollution-free aquaculture, it has been forbidden in some countries. However, malachite green is still illegally employed in fish farming because of its remarkable antibacterial property and low price.

In order to detect whether MG remains in water of aquaculture, it is necessary to develop a rapid and effective method in detecting MG. The most common method is surface-enhanced Raman scattering (SERS),[5–14] but substrate unreliability and impurity interference are major inhibited factors for practical application.[15] In recent years, several publications have reported fluorescence detection method for MG, and some results have been achieved.[16–19] However, only a few lanthanide CP were used to detect MG.[20–22] It is still necessary to develop Ln-CP fluorescent sensors for MG detection with higher selectivity and sensitivity.

Much industrial wastewater discharged from mining, metallurgy, chemical and battery manufacture involves a large amount of toxic heavy metal ions. Heavy metal ion pollution was regarded as severe danger to aquatic organisms, plants, animals, human health and the environment, so it is still a severe task to develop an effective method for detecting heavy metal ions in industrial wastewater. Traditional detection methods for heavy metal ions include ultraviolet spectrometry (UV),[23–29] atomic absorption spectrometry (AAS),[30,31] fluorescence spectrometry (FS),[32–37] and inductively coupled plasma mass spectrometry (ICP-MS).[38–41] Among these methods, fluorescence spectrometry has been used widely because it is simple, fast, precise and cost-effective.[42,43] It is necessary to design new chemical sensors for the efficient detection of trace metal ions in environmental chemistry.

Due to multiple coordination modes and remarkable fluorescence characteristics,[44–53] lanthanide CP (such as Tb-CP, Eu-CP) have been widely employed in fluorescent detection,[54–65] such as detecting metal cations,[66–75] inorganic anions,[69–75] small

[a]*School of Chemistry, Chemical Engineering and Materials, Jining University, Qufu, Shandong, 273155, P. R. China. E-mail: hanlij78@163.com; Tel: +86-25-3196089*

[b]*State Key Laboratory of Coordination Chemistry, School of Chemistry and Chemical Engineering, Nanjing University, Nanjing 210023, P. R. China*

† Electronic supplementary information (ESI) available: The supporting figures are provided. CCDC 2082443. For ESI and crystallographic data in CIF or other electronic format see DOI: 10.1039/d2ra00077f

organic molecules[76–80] and explosives.[81–83] However, it is rarely recorded that lanthanide CP as multifunctional luminescent probe dedicated to detecting MG and various metal ions.[22] In this work, we synthesized an Eu-based CP, $Eu(PDCA)_2(H_2O)_6$ (referred to as Eu-PDCA, PDCA = 2,6-pyridinedicarboxylic acid), and surveyed its application in fluorescence detection. We detected 11 metal cations, 13 anions, six other compounds, and the results showed that Eu-PDCA can rapidly recognize malachite green and cations ($Cr^{3+}$, $Fe^{3+}$ and $Cu^{2+}$) by fluorescence quenching.

## 2. Experimental

### 2.1 Synthesis of $Eu(PDCA)_2(H_2O)_6$

A solution of distilled water (3 mL) containing $Eu(NO_3)_3 \cdot 6H_2O$ (0.0267 g, 0.06 mmol) and 2,6-pyridinedicarboxylic acid (0.0201 g, 0.12 mmol) was placed in a Teflon vessel under autogenous pressure and heated at 140 °C for 96 hours, cooled to room temperature over 48 hours. Yellow block crystals were obtained and washed with distilled water and ethanol, dried in air and collected in 61% yield.

### 2.2 Luminescence sensing experiment

Ethanol solution (50 mL) was added into the ground Eu-PDCA powder (25 mg), performing ultrasonic treatment for four hours. After standing for 12 hours, the colloidal suspension of upper layer was used for fluorescence detection. Malachite green ($5 \times 10^{-4}$ mol $L^{-1}$ in water solution) and other substances or ions ($5 \times 10^{-3}$ mol $L^{-1}$ in water solution) were dropped into Eu-PDCA suspension, respectively, then the photoluminescence (PL) spectroscopy was monitored.

## 3. Results and discussion

### 3.1 Crystal structure

X-ray crystallographic analysis reveals that $Eu(PDCA)_2(H_2O)_6$ (PDCA = 2,6-pyridinedicarboxylic acid) crystallizes in monoclinic system, $P2_1/c$ space group. Eu(III) cation lay in nine coordinated environment, where four oxygen atoms in two carboxylate groups from two 2,6-pyridinedicarboxylic acid ligands, two nitrogen atoms from the same two 2,6-pyridinedicarboxylic acid ligands, one oxygen atom from other 2,6-pyridinedicarboxylic acid ligand, and two oxygen atoms from two water molecules coordinated to same Eu(III) center (Fig. 1a). The four free water molecules lay in the lattice, and they have been omitted for clarity in Fig. 1a. The average Eu–O distance was 2.454 Å, and average Eu–N distance was 2.563 Å. Moreover, Each Eu(III) coordinated unit connected to each other by the bidentate PDCA ligands, resulting a linear chain (Fig. 1b). A three-dimensional structure is achieved by π–π stacking interactions between pyridine rings, as shown in Fig. 1c. The two pyridine rings are stacked in a parallel-displaced geometry with lateral offset. The interplanar distance between the two pyridine rings is 3.231 Å, respectively. The Eu–O bond lengths and bond angles listed in Table S1,† and the crystal data and structural refinement parameters are summarized in Table S2.†

### 3.2 Thermal stability and PXRD

Thermogravimetric analysis (TGA) and powder X-ray diffraction (PXRD) were measured for the thermal and chemical stability analysis. Thermal gravimetric analysis of Eu-PDCA was shown in Fig. S1.† The weight loss rate of first stage was 18.5% (calcd 18.3%) from room temperature to 118 °C, which was responsible for losing all water molecules. The weight loss rate of 52.1% (calcd 55.9%) happened in second stage after 118 °C, belonging to the loss of coordinated 2,6-pyridinedicarboxylic acid. The powder X-ray diffraction displayed that crystal peaks of Eu-PDCA were consistent with simulated patterns, suggesting the pure crystals of Eu-PDCA (Fig. S2†).

### 3.3 Luminescence properties of Eu-PDCA

**3.3.1 Fluorescent detecting MG by Eu-PDCA.** In order to investigate the fluorescence sensing quality of Eu-PDCA, we detected six substances, 11 metal cations and 13 inorganic anions, and the test results of six substances were displayed in Fig. 2.

As shown in Fig. 2a and S3, among the six substances (malachite green, epinephrine bitartrate, ascorbic acid, glucose, L-cysteine, *p*-nitroaniline), only adding 20 μL malachite green ($5 \times 10^{-4}$ mol $L^{-1}$) to Eu-PDCA suspension, the fluorescence intensity of Eu-PDCA was almost reduced to zero, representing complete quenching. However, when 300 μL other substances ($5 \times 10^{-3}$ mol $L^{-1}$) were added to Eu-PDCA suspension respectively, the fluorescence intensity of Eu-PDCA was not completely quenched. Fig. 2b demonstrating the fluorescence spectra of Eu-PDCA (ethanol suspension, 1.0 mL) added various analytes (20 μL), the result also revealed the 20 μL MG had the best quenching ability with small volume and quick response (in seconds), so Eu-PDCA can effectively detect MG by fluorescence quenching.

The detection of MG is performed by measuring fluorescence spectroscopy of Eu-PDCA before and after adding MG. With the dropping of MG, the fluorescence intensity of Eu-PDCA decreased gradually. When adding 20 μL MG, the fluorescence intensity of Eu-PDCA at 615 nm almost decreased to 0. The titration curves for Eu-PDCA by MG are shown in Fig. 3a. The detection was immediately completed when MG was dropped, only spending several seconds. The result revealed malachite green had evident fluorescent quenching ability for Eu-PDCA. The quenching efficiency $K_{sv}$ was calculated by the Stern–Volmer (SV) equation. Fig. 3b presenting the Stern–Volmer plots, the $I_o/I$ is linearly proportional to MG concentration, and the slope is the $K_{sv}$. The $K_{sv}$ for MG was quantified to be $2.10 \times 10^6$ $M^{-1}$, exhibiting excellent selectivity of Eu-PDCA toward MG. Moreover, the calculated detection limit was 0.039 μM. In addition, in order to detect more conveniently and quickly, fluorescence test strip was used for detecting MG. The test strip was prepared by dipping a filter paper ($1 \times 3$ $cm^2$) in Eu-PDCA ethanol suspension and dried at room temperature. As shown in the left of Fig. 3c, the test strip was white under natural light. For the detection of MG, the test strip was dipped in MG aqueous solution for 1 min and exposed to air for drying. Seeing the right of Fig. 3c, the test strip was greenblack after immersed

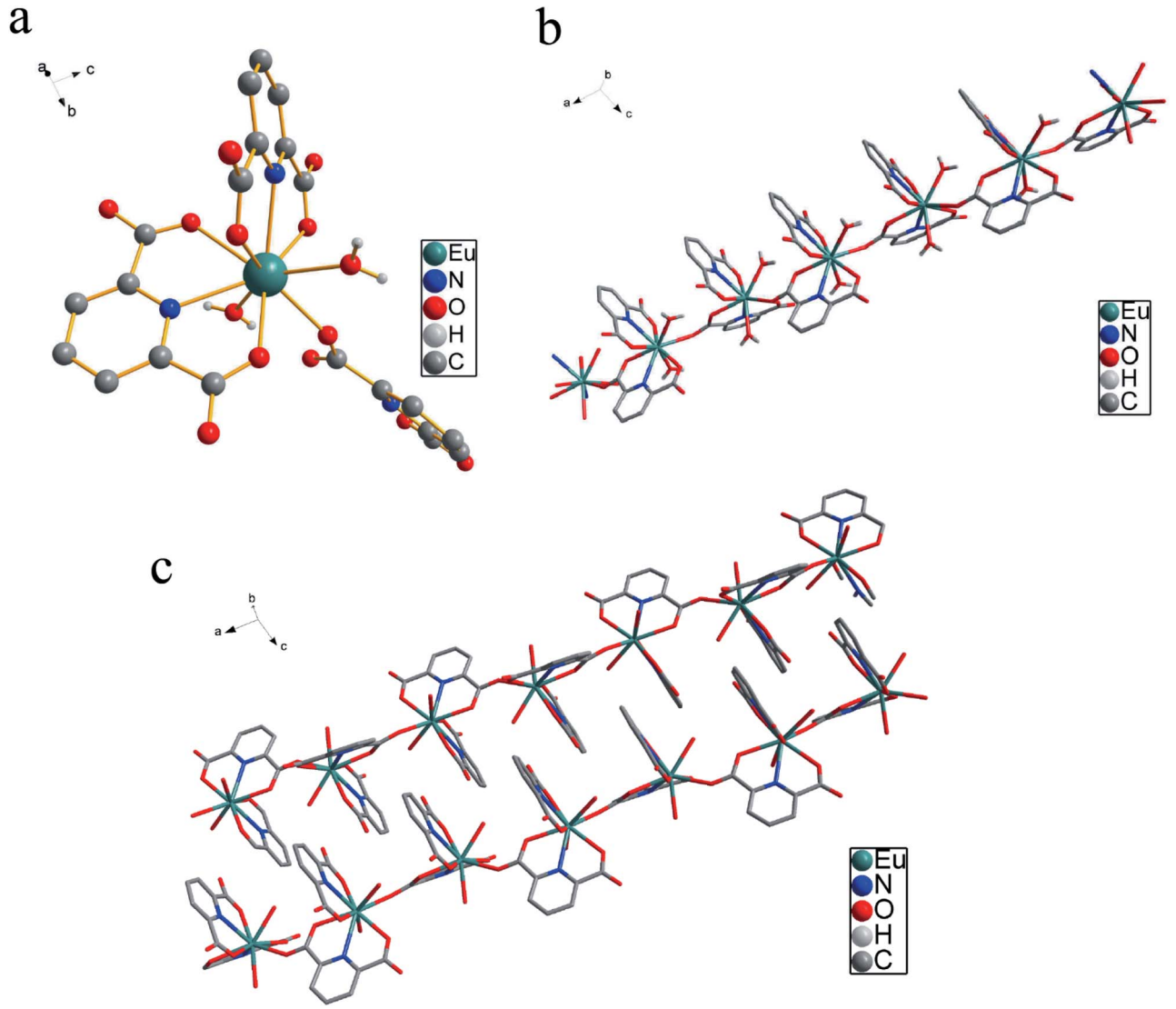


Fig. 1 (a) Coordination mode of Eu(III) cation for Eu-PDCA (four free water molecules were omitted for clarity). (b) A linear chain formed by Eu–O coordinated bonds. (c) 3D structure formed by π–π stacking interactions between pyridine rings.

in MG observed under natural light. In the left of Fig. 3d, under the irradiation of UV light of 365 nm, the test strip without MG was pink. While the pink fluorescence of the test paper disappeared after soaked in MG aqueous solution (in the right of Fig. 3d). To sum up, Eu-PDCA presented fast-responsive luminescent recognition for MG with excellent selectivity and sensitivity.

**3.3.2 Fluorescent detecting cations by Eu-PDCA.** In Fig. 4a and S4, among 11 metal cations, $Cr^{3+}$ (30 μL), $Fe^{3+}$ (40 μL) and $Cu^{2+}$(50 μL) can completely quench the fluorescence of Eu-PDCA. While quench ability for Eu-PDCA by other cations ($Cd^{2+}$, $Zn^{2+}$, $Al^{3+}$, $Ag^{+}$, $K^{+}$, $Ca^{2+}$) was weak, and their quenching ability gradually decreased. $Cd^{2+}$ (200 μL) can quench the 97.2% fluorescence intensity of Eu-PDCA, and $Zn^{2+}$ (300 μL) can quench 96.9% fluorescence intensity of Eu-PDCA. In addition, when $Ba^{2+}$ or $Mg^{2+}$ ions are added dropwise, fluorescence enhancement occurs. $Ba^{2+}$ (130 μL) can enhance the relative fluorescence intensity of Eu-PDCA from 1 to 1.973, and $Mg^{2+}$ (100 μL) enhance the relative fluorescence intensity from 1 to 1.957. But beyond this volume, the fluorescence intensity will decrease slightly. Fig. 4b presenting the fluorescence spectra of Eu-PDCA (ethanol suspension, 1.0 mL) added 40 μL metal cations, when 40 μL $Cr^{3+}$, $Fe^{3+}$ and $Cu^{2+}$ was added, the fluorescence intensity at 615 nm of Eu-PDCA almost reduced to 0, indicating $Cr^{3+}$, $Fe^{3+}$ and $Cu^{2+}$ having excellent quench ability for Eu-PDCA.

As shown in Fig. 5a, d and g, $Cr^{3+}$ (30 μL), $Fe^{3+}$ (40 μL) and $Cu^{2+}$(50 μL) can decrease the relative fluorescence intensity of Eu-PDCA nearly to 0. And calculated $K_{sv}$ for $Cr^{3+}$, $Fe^{3+}$ and $Cu^{2+}$ was $1.46 \times 10^5$ $M^{-1}$, $7.26 \times 10^5$ $M^{-1}$, $3.64 \times 10^5$ $M^{-1}$, respectively. Moreover, the detection limit was about 0.539 μM for $Cr^{3+}$, 0.490 μM for $Fe^{3+}$ and 0.654 μM for $Cu^{2+}$. In addition, fluorescence test paper was also prepared for detecting $Cr^{3+}$, $Fe^{3+}$ and $Cu^{2+}$ cations. As shown in Fig. 5b, e and h, the pictures

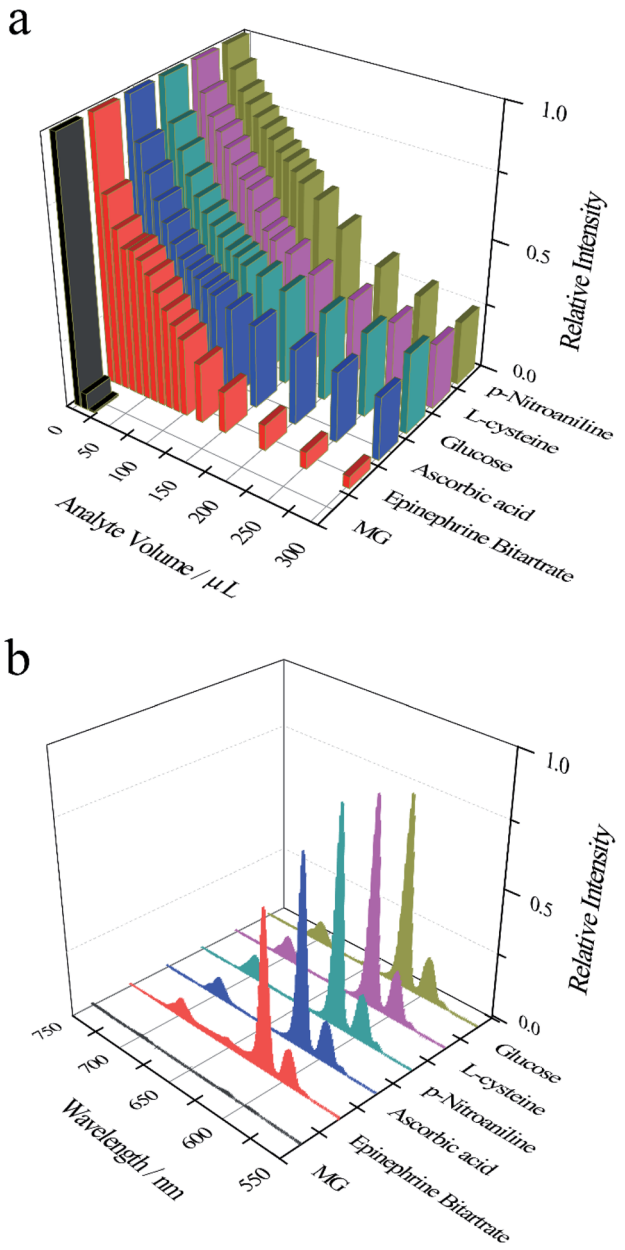


Fig. 2 (a) Bar graph representing the change of the relative emission intensity at 615 nm in the presence of six various analytes. (b) Fluorescence spectra of Eu-PDCA (ethanol suspension, 1.0 mL) added various analytes (20 μL) (excited at 265 nm).

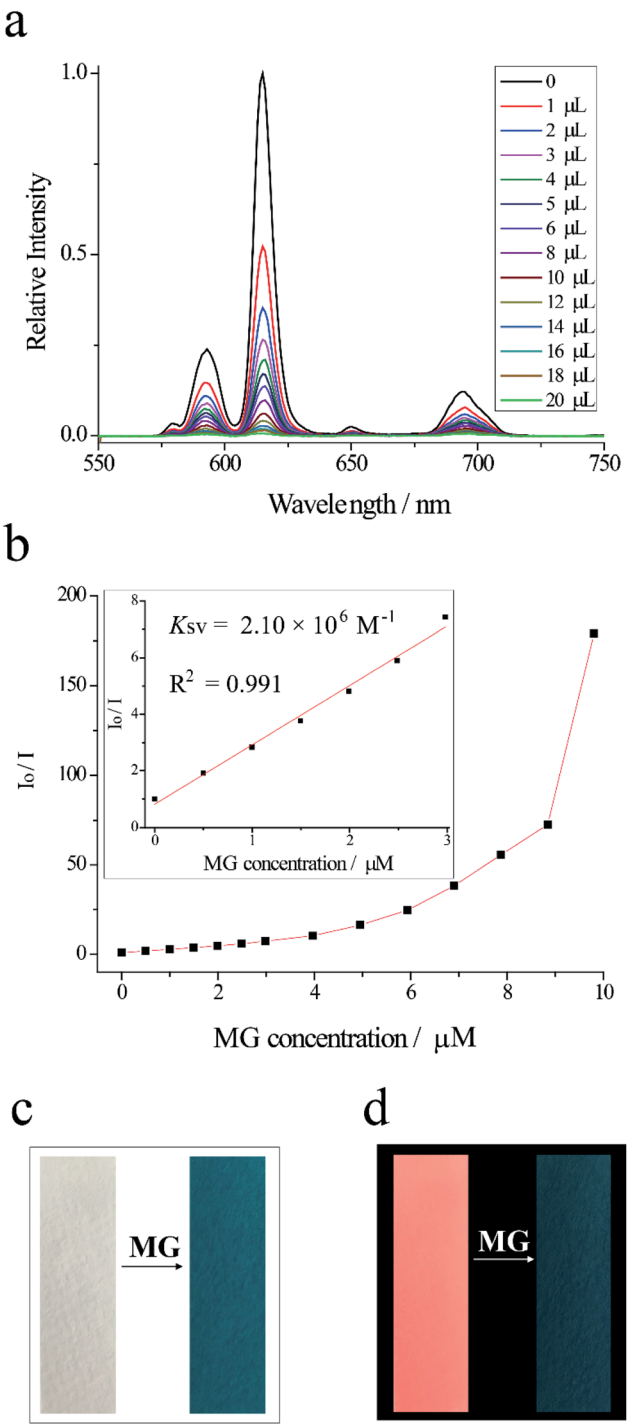


Fig. 3 (a) Fluorescence spectra of Eu-PDCA (ethanol suspension, 1.0 mL) added MG solution ($5 \times 10^{-4}$ mol $L^{-1}$) (excited at 265 nm). (b) SV curve for MG. (c) Optical image of Eu-PDCA test paper after immersed in MG solution under natural light. (d) Optical image of the Eu-PDCA test paper after immersed in MG solution under 365 nm ultraviolet light.

of the test strips before and after soaking in cations solution show almost no change, except that the test strips soaked in iron ions are slightly yellow observed in natural light. Under 365 nm ultraviolet lamp, it was found that the pink fluorescence of the test strips after soaked in solution disappeared (Fig. 5c, f and i). Eu-PDCA can detect $Cr^{3+}$, $Fe^{3+}$ and $Cu^{2+}$ by fluorescence quenching, and fluorescence test strips can help detect $Cr^{3+}$, $Fe^{3+}$ and $Cu^{2+}$ quickly.

**3.3.3 Fluorescent detecting anions by Eu-PDCA.** In Fig. 6a, 6c and S5, among 13 anions, $MnO_4^-$ (30 μL) can completely quench fluorescence of Eu-PDCA, $CrO_4^{2-}$ (300 μL) can quench the 90.6% fluorescence intensity of Eu-PDCA, and $ClO_4^-$ (300 μL) can quench the 51.3% fluorescence intensity of Eu-PDCA. While 300 μL other anions ($BrO_3^-$, $Br^-$, $Cl^-$, $SO_4^{2-}$, $H_2PO_4^-$, $NO_2^-$, $F^-$, $HCO_3^-$, $CH_3COO^-$) processed weaker quench

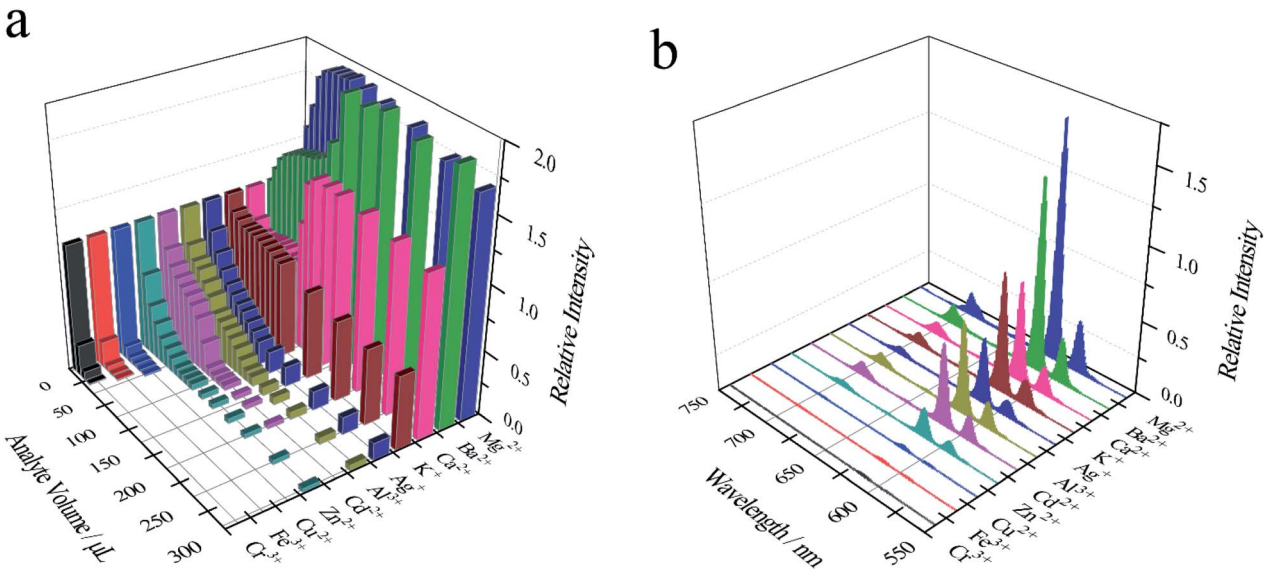


Fig. 4 (a) Bar graph representing the change of the relative emission intensity at 615 nm in the presence of 11 cations. (b) Fluorescence spectra of Eu-PDCA (ethanol suspension, 1.0 mL) added various cations (40 μL) (excited at 265 nm).

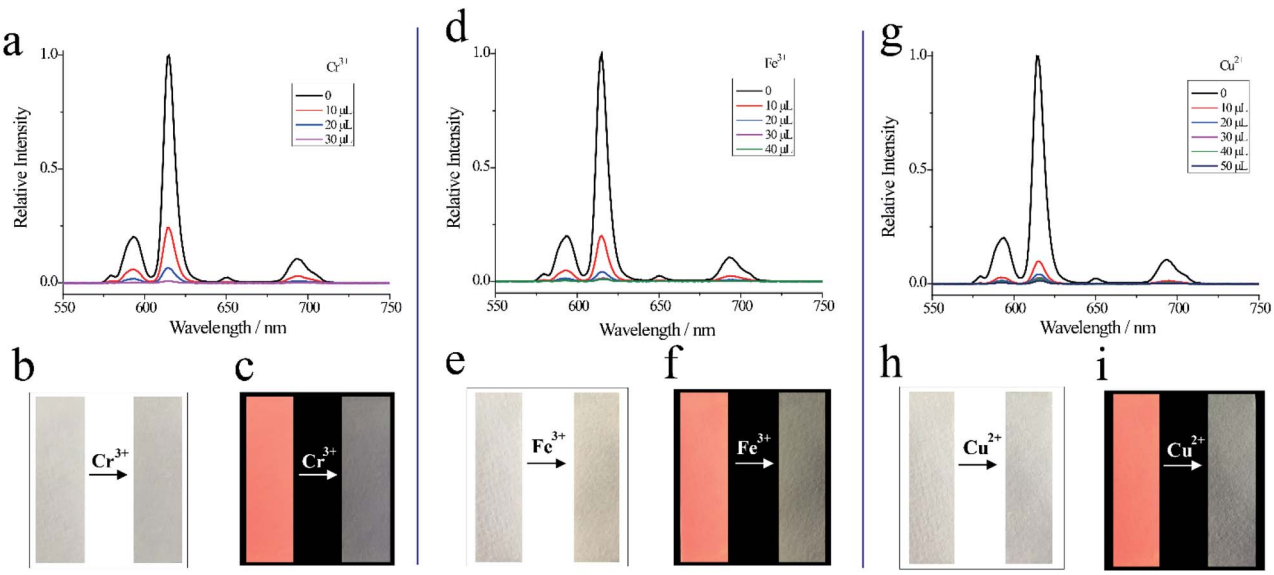


Fig. 5 (a), (d) and (g) Fluorescence spectra of Eu-PDCA (ethanol suspension, 1.0 mL) added metal ions ($5 \times 10^{-3}$ mol $L^{-1}$) (excited at 265 nm). (a) $Cr^{3+}$, (d) $Fe^{3+}$, (g) $Cu^{2+}$. Optical image of Eu-PDCA test paper after immersed in solutions under natural light, (b) $Cr^{3+}$, (e) $Fe^{3+}$, (h) $Cu^{2+}$. Optical image of Eu-PDCA test paper after immersed in solutions under 365 nm ultraviolet light, (c) $Cr^{3+}$, (f) $Fe^{3+}$, (i) $Cu^{2+}$.

ability for Eu-PDCA. In addition, added $PO_4^{3-}$ (50 μL), the relative fluorescence intensity of Eu-PDCA was increased from 1 to 3.557, belong to fluorescence enhancement. However, when the volume of $PO_4^{3-}$ continued to increase, the fluorescence intensity of suspension decreased. Fig. 6b representing the fluorescence spectra of Eu-PDCA (ethanol suspension, 1.0 mL) added 30 μL anions, the result revealed that $MnO_4^-$ (30 μL) has best fluorescence quench effect for Eu-PDCA, and $PO_4^{3-}$ has obvious fluorescence enhancement effect with low concentration.

### 3.4 Detection mechanism

The spectral overlap, energy competition and transfer[32,66,84] were responsible for fluorescent quenching of Eu-PDCA. As can be seen in Fig. S6† of the liquid UV-vis spectra, MG, $Cr^{3+}$, $Fe^{3+}$ and $Cu^{2+}$ in water have wide absorption bands from 200 to 700 nm, which covered the majority absorption band of Eu-PDCA suspension. Under the excitation of light source, there was a competition of absorbing light source energy.[85,86] Therefore,

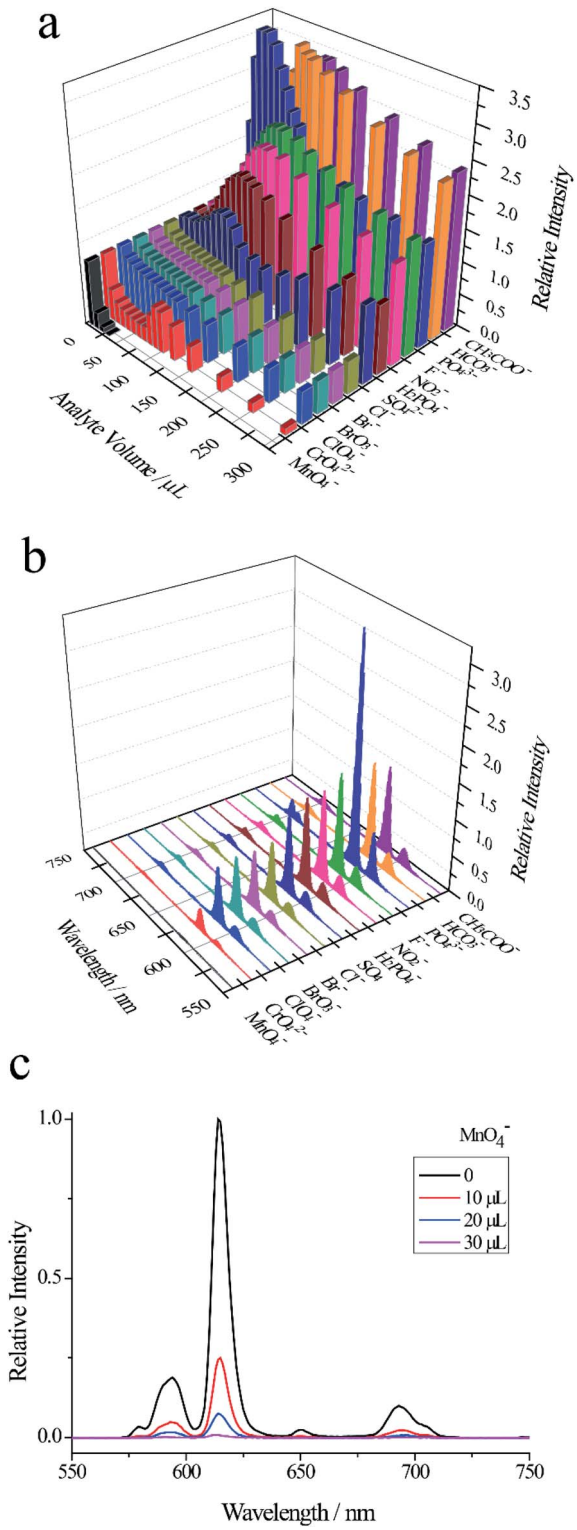


Fig. 6 (a) Bar graph representing the change of the relative emission intensity at 615 nm in the presence of 13 anions. (b) Fluorescence spectra of Eu-PDCA (ethanol suspension, 1.0 mL) added various anions (30 μL) (excited at 265 nm). (c) Fluorescence spectra of Eu-PDCA (ethanol suspension, 1.0 mL) added $MnO_4^-$ ($5 \times 10^{-3}$ mol $L^{-1}$) (excited at 265 nm).

MG, $Cr^{3+}$, $Fe^{3+}$ and $Cu^{2+}$ almost filtered all the light adsorption of Eu-PDCA, leading to the fluorescent quenching.

## 4. Conclusions

We synthesized a europium-based coordination polymer (Eu-PDCA) and surveyed its application in luminescent sensing. Eu-PDCA was capable of quick and effective optical detection of malachite green, cations ($Cr^{3+}$, $Fe^{3+}$ and $Cu^{2+}$) and anion $MnO_4^-$ *via* a luminescence quenching mechanism. Among 11 metal cations, 13 anions, six other substances, Eu-PDCA has high quenching efficiency of $2.10 \times 10^6$ $M^{-1}$ and low detection limit of 0.039 μM for MG. It is hoped that our results can provide new inspiration to design fluorescent sensors for MG and ions.

## Conflicts of interest

There are no conflicts to declare.

## Acknowledgements

This work was financial supported by the National Natural Science Foundation of China (No. 21701048), and the Natural Science Foundation of Shandong Province (ZR2017MB047).

## Notes and references

1 L. Wu, Z. Z. Lin, H. P. Zhong, A. H. Peng, X. M. Chen and Z. Y. Huang, *Food Chem.*, 2017, **229**, 847.
2 R. Sahraei, A. Farmany, S. S. Mortazavi and H. Noorizadeh, *Environ. Monit. Assess.*, 2013, **185**, 5817.
3 S. Srivastava, R. Sinha and D. Roy, *Aquat. Toxicol.*, 2004, **66**, 319.
4 S. L. Stead, H. Ashwin, B. H. Johnston, A. Dallas, S. A. Kazakov, J. A. Tarbin, M. Sharman, J. Kay and B. J. Keely, *Anal. Chem.*, 2010, **82**, 2652.
5 T. Xu, X. Wang, Y. Huang, K. Lai and Y. Fan, *Food Control*, 2019, **106**, 106720.
6 D. Zhang, H. You, L. Yuan, R. Hao, T. Li and J. Fang, *Anal. Chem.*, 2019, **91**, 4687.
7 D. Deng, Q. Lin, H. Li, Z. Huang, Y. Kuang, H. Chen and J. Kong, *Talanta*, 2019, **200**, 272.
8 X. Luo, W. Liu, C. Chen, G. Jiang, X. Hu, H. Zhang and M. Zhong, *Opt. Laser Technol.*, 2021, **139**, 106969.
9 H. Xie, P. Li, J. Shao, H. Huang, Y. Chen, Z. Jiang, P. K. Chu and X.-F. Yu, *ACS Sens.*, 2019, **4**, 2303.
10 X. Zhao, J. Yu, C. Zhang, C. Chen, S. Xu, C. Li, Z. Li, S. Zhang, A. Liu and B. Man, *Appl. Surf. Sci.*, 2018, **455**, 1171.
11 Y. Quan, R. Su, S. Yang, L. Chen, M. Wei, H. Liu, J. Yang, M. Gao and B. Li, *J. Hazard. Mater.*, 2021, **412**, 125209.
12 S. A. Ogundare and W. E. van Zyl, *Colloids Surf. A*, 2019, **570**, 156.
13 W. Fang, X. Zhang, Y. Chen, L. Wan, W. Huang, A. Shen and J. Hu, *Anal. Chem.*, 2015, **87**, 9217.
14 P. Kumar, R. Khosla, M. Soni, D. Deva and S. K. Sharma, *Sens. Actuators, B*, 2017, **246**, 477.

15 D. Chen, X. Zhu, J. Huang, G. Wang, Y. Zhao, F. Chen, J. Wei, Z. Song and Y. Zhao, *Anal. Chem.*, 2018, **90**, 9048.
16 H. Ran, Z. Lin, C. Hong, J. Zeng, Q.-H. Yao and Z.-Y. Huang, *J. Photochem. Photobiol., A*, 2019, **372**, 260.
17 Y. J. Ju, N. Li, S. G. Liu, L. Han, N. Xiao, H. Q. Luo and N. B. Li, *Sens. Actuators, B*, 2018, **275**, 244.
18 W. Gui, H. Wang, Y. Liu and Q. Ma, *Sens. Actuators, B*, 2018, **266**, 685.
19 L. Wu, Z. Lin, H. Zhong, X. Chen and Z. Huang, *Sens. Actuators, B*, 2017, **239**, 69.
20 X. Zhang, Y. Li and L. Zhang, *Spectrochim. Acta A*, 2021, **251**, 119464.
21 K. Yi and L. Zhang, *Food Chem.*, 2021, **354**, 129584.
22 L.-J. Han, Y.-J. Kong, G.-Z. Hou, H.-C. Chen, X.-M. Zhang and H.-G. Zheng, *Inorg. Chem.*, 2020, **59**, 7181.
23 F. Amourizi, K. Dashtian, M. Ghaedi and B. Hosseinzadeh, *Anal. Methods*, 2021, **13**, 2603.
24 J. Wang, J. Wu, Y. Zhang, X. Zhou, Z. Hu, X. Liao, B. Sheng, K. Yuan, X. Wu, H. Cai, H. Zhou and P. Sun, *Sens. Actuators, B*, 2021, **330**, 129364.
25 B. Unnikrishnan, C.-W. Lien, H.-W. Chu and C.-C. Huang, *J. Hazard. Mater.*, 2021, **401**, 123397.
26 Y. Guo, C. Liu, R. Ye and Q. Duan, *Appl. Sci.*, 2020, **10**, 6874.
27 J. Yang, Y. Zhang, J. Guo, Y. Fang, Z. Pang and J. He, *ACS Appl. Mater. Interfaces*, 2020, **12**, 39118.
28 X. She, H. Xu, Y. Xu, J. Yan, J. Xia, L. Xu, Y. Song, Y. Jiang, Q. Zhang and H. Li, *J. Mater. Chem. A*, 2014, **2**, 2563.
29 J. Du, Y. Sun, L. Jiang, X. Cao, D. Qi, S. Yin, J. Ma, F. Y. C. Boey and X. Chen, *small*, 2011, **7**, 1407.
30 M. Ghaedi, F. Ahmadi and A. Shokrollahi, *J. Hazard. Mater.*, 2007, **142**, 272.
31 J. A. Baig, T. G. Kazi, M. B. Arain, H. I. Afridi, G. A. Kandhro, R. A. Sarfraz, M. K. Jamal and A. Q. Shah, *J. Hazard. Mater.*, 2009, **166**, 662.
32 L.-J. Han, W. Yan, S.-G. Chen, Z.-Z. Shi and H.-G. Zheng, *Inorg. Chem.*, 2017, **56**, 2936.
33 H. N. Kim, W. X. Ren, J. S. Kim and J. Yoon, *Chem. Soc. Rev.*, 2012, **41**, 3210.
34 L. N. Neupane, E.-T. Oh, H. J. Park and K.-H. Lee, *Anal. Chem.*, 2016, **88**, 3333–3340.
35 G. Yang, X. Wan, Y. Su, X. Zeng and J. Tang, *J. Mater. Chem. A*, 2016, **4**, 12841.
36 A. K. Saini, M. Srivastava, V. Sharma, V. Mishra and S. M. Mobin, *Dalton Trans.*, 2016, **45**, 3927.
37 X. Guo, D. Xu, H. Yuan, Q. Luo, S. Tang, L. Liu and Y. Wu, *J. Mater. Chem. A*, 2019, **7**, 27081.
38 M. Ghaedi, F. Ahmadi and A. Shokrollahi, *J. Hazard. Mater.*, 2007, **142**, 272.
39 J. Qin, Z. Su, Y. Mao, C. Liu, B. Qi, G. Fang and S. Wang, *Ecotoxicol. Environ. Saf.*, 2021, **208**, 111729.
40 X. Fu, E. Chen, B. Ma, Y. Xu, P. Hao, M. Zhang, Z. Ye, X. Yu, C. Li and Q. Ji, *Foods*, 2021, **10**, 413.
41 E. M. Krupp, B. F. Milne, A. Mestrot, A. A. Meharg and J. Feldmann, *Anal. Bioanal. Chem.*, 2008, **390**, 1753.
42 Y.-W. Li, J. Li, X.-Y. Wan, D.-F. Sheng, H. Yan, S.-S. Zhang, H.-Y. Ma, S.-N. Wang, D.-C. Li, Z.-Y. Gao, J.-M. Dou and D. Sun, *Inorg. Chem.*, 2021, **60**, 671.
43 Y. Lu, Y. Liang, Y. Zhao, M. Xia, X. Liu, T. Shen, L. Feng, N. Yuan and Q. Chen, *ACS Appl. Mater. Interfaces*, 2021, **13**, 1644.
44 Y. Cui, H. Xu, Y. Yue, Z. Guo, J. Yu, Z. Chen, J. Gao, Y. Yang, G. Qian and B. Chen, *J. Am. Chem. Soc.*, 2012, **134**, 3979.
45 X. Rao, T. Song, J. Gao, Y. Cui, Y. Yang, C. Wu, B. Chen and G. Qian, *J. Am. Chem. Soc.*, 2013, **135**, 15559.
46 Y. Wan, J. Wang, H. Shu, B. Cheng, Z. He, P. Wang and T. Xia, *Inorg. Chem.*, 2021, **60**, 7345.
47 E. H. Otal, H. Tanaka, M. L. Kim, J. P. Hinestroza and M. Kimura, *Chem. - Eur. J.*, 2021, **27**, 7376.
48 M. Hu, Y. Shu, A. Kirillov, W. Liu, L. Yang and W. Dou, *ACS Appl. Mater. Interfaces*, 2021, **13**, 7625.
49 D. A. Gálico, A. A. Kitos, J. S. Ovens, F. A. Sigoli and M. Murugesu, *Angew. Chem., Int. Ed.*, 2021, **60**, 6130.
50 T. Gorai, W. Schmitt and T. Gunnlaugsson, *Dalton Trans.*, 2021, **50**, 770.
51 J.-M. Wang, P.-F. Zhang, J.-G. Cheng, Y. Wang, L.-L. Ma, G.-P. Yang and Y.-Y. Wang, *CrystEngComm*, 2021, **23**, 411.
52 V. Trannoy, A. N. Carneiro Neto, C. D. S. Brites, L. Carlos and H. Serier-Brault, *Adv. Opt. Mater.*, 2021, **9**, 2001938.
53 F. Saraci, V. Quezada-Novoa, P. Rafael Donnarumma and A. J. Howarth, *Chem. Soc. Rev.*, 2020, **49**, 7949.
54 Y. Cui, Y. Yue, G. Qian and B. Chen, *Chem. Rev.*, 2012, **112**, 1126.
55 Y. Cui, B. Chen and G. Qian, *Coord. Chem. Rev.*, 2014, **273**, 76.
56 M. D. Allendorf, C. A. Bauer, R. K. Bhakta and R. J. T. Houk, *Chem. Soc. Rev.*, 2009, **38**, 1330.
57 F.-Y. Yi, D. Chen, M.-K. Wu, L. Han and H.-L. Jiang, *ChemPlusChem*, 2016, **81**, 675.
58 K. A. White, D. A. Chengelis, K. A. Gogick, J. Stehman, N. L. Rosi and S. Petoud, *J. Am. Chem. Soc.*, 2009, **131**, 18069.
59 B. Yan, *Acc. Chem. Res.*, 2017, **50**, 2789.
60 P. Zhang, N. Song, S. Liu, Q. Li, Y. Wang and B. Zhou, *J. Mater. Chem. C*, 2021, **9**, 6208.
61 J. Liu, X. Han, Y. Lu, S. Wang, D. Zhao and C. Li, *Inorg. Chem.*, 2021, **60**, 4133.
62 T. Xia, Y. Wan, X. Yan, L. Hu, Z. Wu and J. Zhang, *Dalton Trans.*, 2021, **50**, 2792.
63 Y.-Q. Sun, Y. Cheng and X.-B. Yin, *Anal. Chem.*, 2021, **93**, 3559.
64 K. Yin, S. Wu, H. Zheng, L. Gao, J. Liu, C. Yang, L.-W. Qi and J. Peng, *Langmuir*, 2021, **37**, 5321.
65 Y.-J. Tong, L.-D. Yu, J. Zheng, G. Liu, Y. Ye, S. Huang, G. Chen, H. Yang, C. Wen, S. Wei, J. Xu, F. Zhu, J. Pawliszyn and G. Ouyang, *Anal. Chem.*, 2020, **92**, 15550.
66 L. J. Han, Y.-J. Kong, X.-M. Zhang, G.-Z. Hou, H.-C. Chen and H.-G. Zheng, *J. Mater. Chem. C*, 2021, **9**, 6051.
67 Q. Lin, W. Xie, Z. Zong, Z. Liu, Y. Sun and L. Liang, *New J. Chem.*, 2021, **45**, 7382.
68 Z.-G. Lin, F.-Q. Song, H. Wang, X.-Q. Song, X.-X. Yu and W. Liu, *Dalton Trans.*, 2021, **50**, 1874.
69 Y. Shu, Q. Ye, T. Dai, Q. Xu and X. Hu, *ACS Sens.*, 2021, **6**, 641.
70 L. Yu, L. Feng, L. Xiong, S. Li, Q. Xu, X. Pan and Y. Xiao, *ACS Appl. Mater. Interfaces*, 2021, **13**, 11646.

71 B. Li, J.-P. Dong, Z. Zhou, R. Wang, L.-Y. Wang and S.-Q. Zang, *J. Mater. Chem. C*, 2021, **9**, 3429.
72 J.-P. Dong, B. Li, Y.-J. Jin and L.-Y. Wang, *CrystEngComm*, 2021, **23**, 1677.
73 J. Jin, J. Xue, Y. Liu, G. Yang and Y.-Y. Wang, *Dalton Trans.*, 2021, **50**, 1950.
74 M. Wang, Z. Liu, X. Zhou, H. Xiao, Y. You and W. Huang, *Inorg. Chem.*, 2020, **59**, 18027.
75 L.-J. Liu, M.-Y. Zhang, Q.-Z. Guo, Z.-H. Zhang and J.-F. Guo, *Dalton Trans.*, 2021, **50**, 1697.
76 W.-P. Ma and B. Yan, *Dalton Trans.*, 2020, **49**, 15663.
77 X.-J. Che, S.-L. Hou, Y. Shi, G.-L. Yang, Y.-L. Hou and B. Zhao, *Dalton Trans.*, 2019, **48**, 3453.
78 H.-Y. Zheng, X. Lian, S.-j. Qin and B. Yan, *Dalton Trans.*, 2018, **47**, 6210.
79 W. Yan, C. Zhang, S. Chen, L. Han and H. Zheng, *ACS Appl. Mater. Interfaces*, 2017, **9**, 1629.
80 H. Wang, J. Qin, C. Huang, Y. Han, W. Xu and H. Hou, *Dalton Trans.*, 2016, **45**, 12710.
81 D. Tian, Y. Li, R.-Y. Chen, Z. Chang, G.-Y. Wang and X.-H. Bu, *J. Mater. Chem. A*, 2014, **2**, 1465.
82 F. G. Moscoso, J. Almeida, A. Sousaraei, T. Lopes-Costa, A. G. Silva, J. Cabanillas-Gonzalez, L. Cunha-Silva and J. Pedrosa, *J. Mater. Chem. C*, 2020, **8**, 3626.
83 Z. Zhan, X. Liang, X. Zhang, Y. Jia and M. Hu, *Dalton Trans.*, 2019, **48**, 1786.
84 Z. Hu, W. P. Lustig, J. Zhang, C. Zheng, H. Wang, S. J. Teat, Q. Gong, N. D. Rudd and J. Li, *J. Am. Chem. Soc.*, 2015, **137**, 16209.
85 S. Nagarkar, B. Joarder, A. K. Chaudhari, S. Mukherjee and S. K. Ghosh, *Angew. Chem., Int. Ed.*, 2013, **52**, 2881.
86 Z. Hu, K. Tan, W. P. Lustig, H. Wang, Y. Zhao, C. Zheng, D. Banerjee, T. J. Emge, Y. J. Chabal and J. Li, *Chem. Sci.*, 2014, **5**, 4873.